Journal of Thermal Analysis and Calorimetry, Vol. 67 (2002) 305–312

THERMAL DECOMPOSITION KINETICS OF POLYURETHANE-COMPOSITES WITH BAGASSE OF SUGAR CANE

C. G. Mothé[1*], *C. R. de Araujo*[1], *M. A. de Oliveira*[2] *and M. I. Yoshida*[2]

[1]Departamento de Processos Orgânicos/Escola de Química/Universidade Federal do Rio de Janeiro, CEP: 21949-900, RJ, Brazil
[2]Departamento de Química/Instituto de Ciências Exatas/Universidade Federal de Minas Gerais, CEP: 31270-901, MG, Brazil

Abstract

Polyurethane composites with bagasse of sugar cane (BSC) at different proportions: 5, 10 and 20 mass/mass% were prepared by melt mixing method. The thermal behavior of these composites were studied by thermogravimetry (TG/DTG). The influence of fiber concentration on the kinetic parameters of the composites was studied and a better interaction was suggested between PU/BSC with 5 mass/mass% of fiber. Scanning electron microscopy was carried out to investigate surface morphology.

Keywords: bagasse of sugar cane, composites, kinetic, polyurethane, thermogravimetry

Introduction

The use of natural fibers like bagasse of sugar cane, coir, sisal, jute, ramie and pineapple-leaf to reinforce plastics offers a number of advantages over conventional materials because of their low cost, biodegradability, flexibility and low gravimetric density. In addition, they are obtained from renewable sources and can improve properties and at the same time can lead to materials which cause less environmental impact [1–3].

The properties of short-fiber composites depend not only upon the matrix and fiber characteristics. The interfacial bonding strength plays an important role in determining the performance of the composite. Several such treatments have been developed to improve the interfacial bonding, as silanes, isocyanates, benzoyl peroxide, dicumyl peroxide and potassium permanganate which improve mechanical properties [4–5].

Bagasse is a by-product of the sugar cane industry, consisting of the sheath and pith material from sugar cane stalk. It consists basically of cellulose but also contains hemicellulose, lignin, some residual sugars, pentosans, hexosans, and other reactive low molecular products [6]. A small percentage of inorganic silica is also present that contributes to inherent fire retardant properties. Bagasse fiber resembles cotton fiber

---

[*] Author for correspondence: E-mail: cheila@eq.ufrj.br

1418–2874/2002/ $ 5.00

Akadémiai Kiadó, Budapest
Kluwer Academic Publishers, Dordrecht

in spiral structure with length in the range of 1–4 and width of 0.01–0.04 mm. Large quantities of bagasse are available in tropic countries such as India, Pakistan, Indonesia, Philippines and Brazil [7].

This work reports the effect of fiber concentration on thermal degradation of polyurethane composites reinforced with bagasse of sugar cane.

Experimental

Materials

The commercial polyurethane pellets were supplied by Cofade – Sociedade Fabricadora de Elastômeros. Bagasse of sugar cane (BSC), an industrial sugar cane reject, was supplied by Usina Paraíso.

Composites

The composites of polyurethane pellets and bagasse of sugar cane with different proportion such as: 5, 10 and 20% by mass of fibers, were prepared by the melt mixing method, in a Haake rheometer, at 100°C, 60 rpm for 15 min. These samples were cured in a carver press at 140°C and 10 000 lb/in^2.

TG measurements

Thermogravimetric studies were carried out on a Mettler TG50 thermobalance of TA4000 system, in nitrogen flow at a rate of 200 mL min^{-1}, by isothermal and non-isothermal heating techniques. The amount of sample used was approximately 5 mg, except for the PU from Cofade (~25 mg).

The non-isothermal curves were obtained at a heating rate of 10°C min^{-1}. The isothermal experiments were performed in the following temperature range: 240–270 for the bagasse of sugar cane, 284–300°C for the PU/BSC with 5% of fiber, 280–300°C for PU/BSC with 10% of fiber, 280–295°C for PU/BSC with 20% of fiber and 284–320°C for PU from Cofade.

Microscopy measurements

The tensile fracture surfaces of the composites were examined under a scanning electron microscopy (SEM), Jeol model JSM 5300.

Results and discussion

Figure 1 depicts thermogravimetric (TG) curves for BSC, PU and PU/BSC composites with different proportions of fiber. All curves present three decomposition stages, except for the PU commercial. The first mass loss for PU commercial sample occurred at T_{onset} 315°C and a residue of 4%. The first mass loss shows that BSC has 10% of water. The composites exhibited similar thermal behavior, with decomposi-

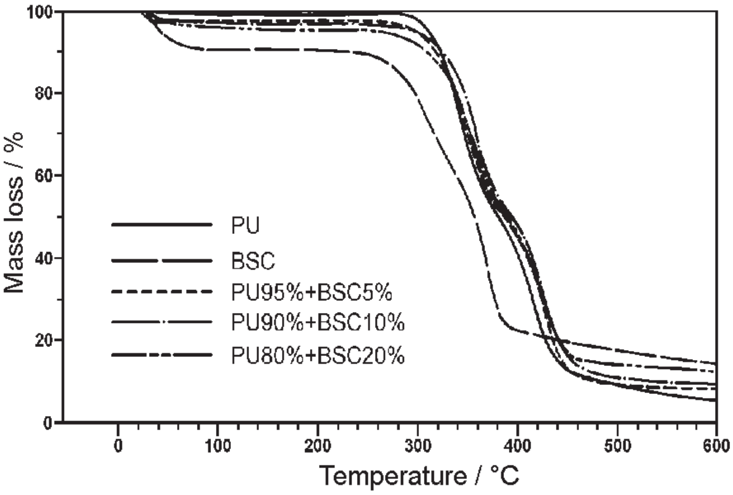

Fig. 1 Thermogravimetric curves for BSC, PU and PU/BSC composites

tion at around 310°C and a residue of 8.4% (PU95%+BSC5%), 9.4% (PU90%+BSC10%), and 12.1% (PU80%+BSC20%).

Derivative thermogravimetric (DTG) curves in Fig. 2 show a major thermal stability for composites with 5% of BSC, according with TG analysis.

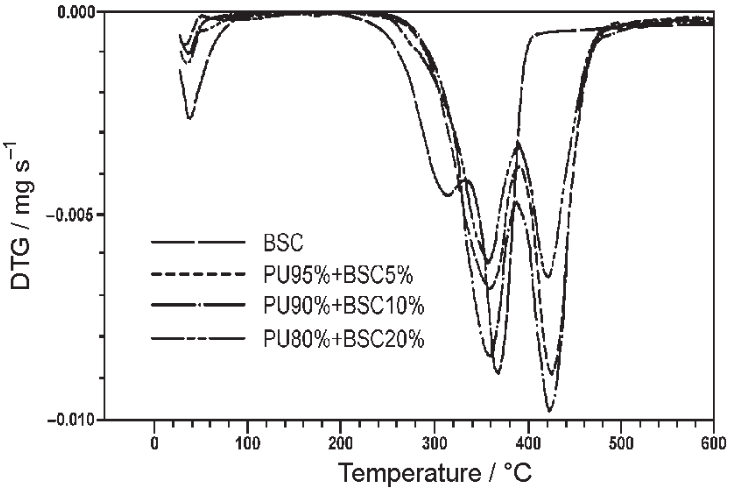

Fig. 2 Derivative thermogravimetric curves for BSC and PU/BSC composites

Under isothermal conditions, the fractional reaction-time (α-t) curves are expressed in the form:

$$g(\alpha)=kt \tag{1}$$

where k is the rate constant and the function $g(\alpha)$ depends on the mechanism controlling the reaction [8–10]. The decomposition fractions, α, were determined by:

$$\alpha = \frac{m_i - m_t}{m_i - m_f} \tag{2}$$

where m_i – initial mass, m_t – mass in time t and m_f – final mass.

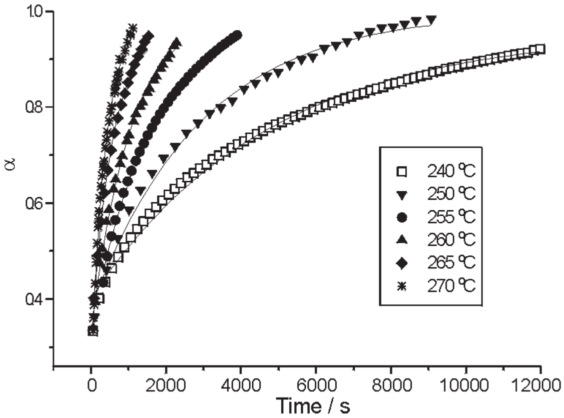

Fig. 3 F_1 plot for the isothermal decomposition of BSC

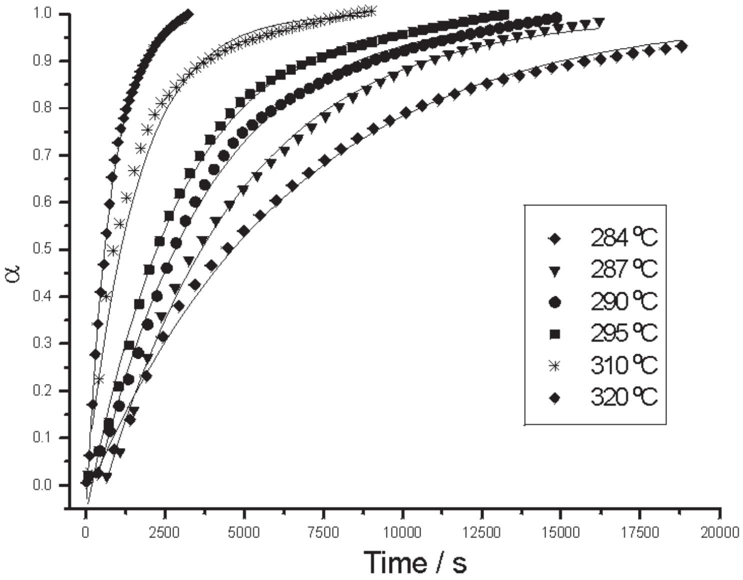

Fig. 4 F_1 plot for the isothermal decomposition of PU commercial

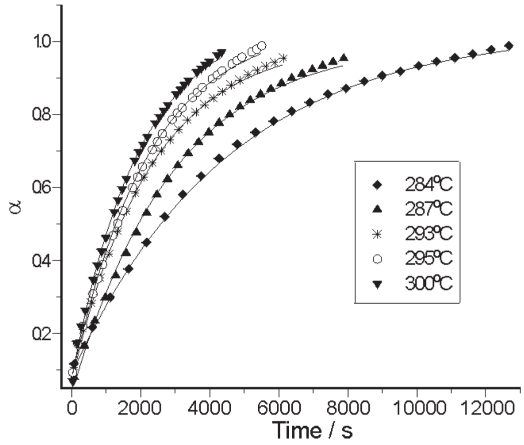

Fig. 5 F_1 plot for the isothermal decomposition of PU commercial PU95%+BSC5%

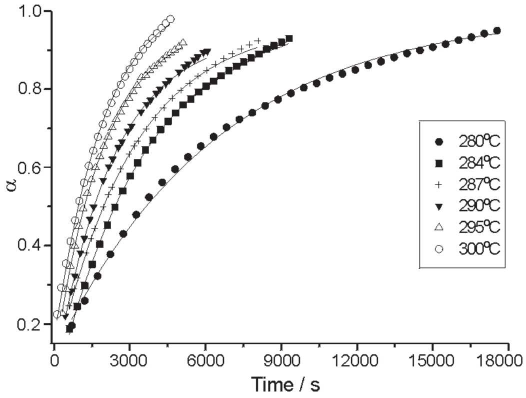

Fig. 6 F_1 plot for the isothermal decomposition of PU commercial PU90%+BSC10%

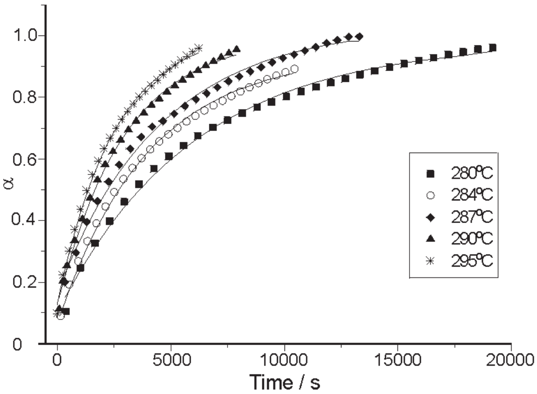

Fig. 7 F_1 plot for the isothermal decomposition of PU80%+BSC20%

Table 1 Kinetic functions $g(\alpha)$ for heterogeneous solid-state reactions

$g(\alpha)=kt$	Symbol	Rate controlling process
Deceleratory α–*t* curves		
a) Based on diffusion mechanism		
α^2	D_1	One-dimensional diffusion
$\alpha+(1-\alpha)\ln(1-\alpha)$	D_2	Two-dimensional diffusion
$[1-(1-\alpha)^{1/3}]^2$	D_3	Three-dimensional diffusion
$1-(2/3)\alpha-(1-\alpha)^{2/3}$	D_4	Three-dimensional diffusion (Gistling-Brounshtein equation)
b) Based on geometrical models		
$1-(1-\alpha)^{1/n}$	R_n	Phase-boundary reaction; *n*=1, 2, and 3 (one, two and three dimensional, respectively)
c) Based on 'order' of reaction		
$-\ln(1-\alpha)$	F_1	First order (Mampel equation)

Table 2 Linear correlation coefficients, *r*, and standard deviations, *s*, to fit equation F_1

Compound	*T*/°C	*r*	*s*
BSC	240	0.9936	0.054
	250	0.9941	0.057
	255	0.9974	0.048
	260	0.9965	0.052
	265	0.9977	0.045
	270	0.9974	0.043
PU	284	0.9975	0.036
	287	0.9977	0.036
	290	0.9968	0.041
	295	0.9963	0.044
	310	0.9920	0.117
	320	0.9984	0.032
PU95%+BSC5%	284	0.9997	0.013
	287	0.9986	0.025
	290	0.9994	0.017
	295	0.9990	0.022
	300	0.9991	0.019
PU90%+BSC10%	280	0.9981	0.034
	284	0.9996	0.014
	287	0.9994	0.016
	290	0.9992	0.021
	295	0.9995	0.014
	300	0.9979	0.037
PU80%+BSC20%	280	0.9962	0.046
	284	0.9961	0.043
	287	0.9930	0.062
	290	0.9981	0.029
	295	0.9987	0.024

Table 3 Kinetic parameters of isothermal degradation of PU, BSC and PU/BSC composites

Composition	E_a/kJ mol^{-1}	A/s^{-1}
PU	151.9	$2.98 \cdot 10^{10}$
BSC	219.3	$3.37 \cdot 10^{18}$
PU95%+BSC5%	94.6	$2.26 \cdot 10^{6}$
PU90%+BSC10%	106.5	$2.94 \cdot 10^{6}$
PU80%+BSC20%	137.4	$1.74 \cdot 10^{6}$

The mechanisms controlled by diffusion, phase-boundary reaction and the model F_1 are compatible with our experimental data and are listed in Table 1. The corresponding kinetic equations were treated by a linear regression program; values of the correlation coefficients and standard deviations (Table 2) were used as a measure of the linearity for the least squares fitting in these $g(\alpha)$ *vs*. t plots. The linear correlation coefficients and standard deviations suggest that the F_1 model is the most appropriate to describe the experimental results (Figs 3–7)

Values for activation energy and pre-exponential factor are shown in Table 3. The activation energy is higher for BSC, followed by PU matrix and PU/BSC composites. The composite with 5% of BSC, showed minor activation energy.

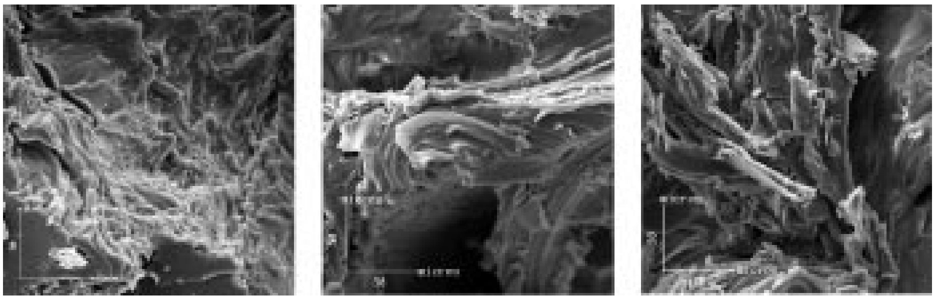

Fig. 8 SEM analysis of fracture region from tensile tests: a – PU95%+BSC5%; b – PU90%+BSC10% and c – PU80%+BSC20%. Magnification: 500×

SEM micrographs of the fracture region from tensile tests are shown in Fig. 8 (a), (b) and (c) for PU/BSC composites with 5, 10 and 20% respectively. The fracture surface presents a homogeneous aspect, but with holes and fiber damage. This may be attributed to the processing in Haake Rheometer.

Conclusions

The isothermal decomposition kinetic studies of BSC, PU commercial and the composites of PU/BSC show that all these compounds follow a same kinetic model, F_1, in the full range of studied temperatures. The deceleratory α–t curves are adequately fitted to the equation $-\ln(1-\alpha)=k$ that corresponds to nucleation and nuclei growth mechanism. The E_a values show that the thermal stability of the composites decreases in the order:

$$\text{PU80\%+BSC20\%} > \text{PU90\%+BSC10\%} > \text{PU95\%+BSC5\%}.$$

The composite with 5% of BSC (E_a 94.6 kJ mol^{-1}) exhibited the best performance with respect to thermal stability, suggesting a better fiber matrix interaction. These data are corroborated with scanning electron microscopy.

* * *

The authors wish to thank CAPES, for financial support.

References

1 de Araujo and C. G. Mothé, Second International Symposium on Natural Polymer and Composites (ISNAPOL/98), SP, Brazil, 1998 p. 123.
2 C. G. Mothé and C. R. de Araujo, 26th Conference North American Thermal Analysis (NATAS), Cleveland, USA 1998, p. 260.
3 C. G. Mothé and C. R. de Araujo, Thermochim. Acta, 358 (2000) 321.
4 K. Joseph, S. Thomas and C. Pavithran, Polymer, 37 (1996) 5139.
5 J. M. Felix and P. Gatenholm, J. Appl. Polym. Sci., 42 (1991) 609.
6 A. M. Usmani and I. O. Salyer, Bagasse-Rubber composite Technology, in Use of Renewable Resources for Polymer Applications, C. E. Carraher and L. H. Sperling, Eds., Plenum Press, New York 17 (1982) 73.
7 M. B.Amin, A. G. Maadhah and A. M. Usmani, Newer Applications of Bagasse, in Use of Renewable Resources for Polymer Applications, C. E. Carraher and L. H. Sperling, Eds., Plenum Press, New York, 33 (1986) 75.
8 D. Dollimore, Thermochim. Acta, 203 (1992) 7.
9 J. M. Criado, M. Gonzalez, A. Ortega and C. Real, Thermochim. Acta, 29 (1984) 243.
10 R. G. Ferrillo and A. Granzow, J. Thermal Anal., 29 (1984) 1237.